ARTICLE

Novel biocompatible electrospun gelatin fibers mat with antibiotic drug delivery properties

Received 00th January 2015,
Accepted 00th January 2015

DOI: 10.1039/x0xx00000x

www.rsc.org/

Sakthivel Nagarajan[a,b], Laurence Soussan[a], Mikhael Bechelany[a], Catherine Teyssier[c], Vincent Cavaillès[c], Céline Pochat-Bohatier[a], Philippe Miele[a], Narayana Kalkura[b], Jean-Marc Janot[a], and Sébastien Balme[a]*

The aim of this study was to synthesize stable gelatin electrospun mats (ESM) (cross-linked by Glutaraldehyde (GTA) vapors) with tunable drug release properties using pH as a stimuli. Gelatin ESM loaded with rhodamine as a model drug was first synthesized. The *in vitro* release of rhodamine was characterized to understand the mechanisms of drug release and the effects of both cross-linker concentration and pH on the drug release. An optimal cross-linker concentration of 5 % was evidenced to provide ESM allowing both sustainable release of drugs at pH 7 and burst release at pH 2. The release profiles were then fitted with a power law model to describe the release kinetic. Chlorhexidine antibiotic drug was finally loaded into the optimal electrospun mat and its bactericidal activity was demonstrated against Gram-negative (*E. coli*) and Gram-positive (*S. epidermidis*) bacteria by agar diffusion tests. This material was shown to efficiently destroy bacterial biofilms and prevent bacterial growth within a short time (3 h), while maintaining its antibacterial activity up to at least 72 h. This study provides a promising material, which could treat infected sites and prevent infections, with tunable drug releasing property using pH as a stimulus.

Introduction,

In recent years, polymer composites, metallic and nonmetallic nanoparticles, dendrimers, micelles, and stimuli responsive polymers have been elaborated and analyzed for drug and biomolecule delivery applications.[1-5] Proteins, polyamino-acids and polysaccharides are widely used biopolymers for biomaterial fabrication. Among this, gelatin is a biopolymer composed by denatured collagen. It consists of repeated units of amino acid sequences, glycine-X-Y (X-proline, Y-hydroxy proline).[6] Since, it is extracted from acid or basic hydrolysis of skin or tendon, it is worth noting that this biopolymer is cheap, abundant and approved as a non-toxic material by the Food and Drug Administration (FDA). The food grade gelatin is rich with Type A (80%) and less Type B (15%). Gelatin does not express antigenicity and is highly resorbable.[7, 8] It is highly degradable by a protease, such as collagenase.[9] Due to all these properties, gelatin nanoparticles loaded with drugs appeared to be useful in the field of drug delivery for anti-cancer, anti-HIV, antimicrobial, analgesic, anti-inflammatory and anti-diabetic drugs release applications[10-15]. Nevertheless, gelatin is highly water soluble, hence it requires stabilization using various types of cross-linkers; such as glutaraldehyde (GTA), ethylene diamine carbodiimide, genipin and N-hydroxy succinimide.[7, 13, 16] Electrospun mats (ESM) are functioning as a biomimetic extra-cellular matrix which provokes the biological activity by acting as a supporting scaffold or drug carriers [17]. Absorption and release of drugs can be thus controlled by localizing it in ESM. In addition, high surface area of the ESM makes them suitable materials for drug delivery applications. It was demonstrated that Poly(lactic-co-glycolic acid)/gelatin based ESM are suitable drug delivery carriers for the release drugs such as fenbufen and doxorubicin.[18, 19] The drug release from the ESM was also controlled by triaxial electrospinning system. Yu *et al.* reported the confinement of drugs at various levels using triaxial electrospinning system and attained zero order drug release of ketoprofen, a nonsteroidal anti-inflammatory agent[20]. The sustained drug release is very essential for implantable ESM. Xhao *et al.* developed an interfacial layer on silica nanoparticles loaded with an anticancer drug and dispersed them in a polymer loaded with an anti-inflammatory drug to fabricate the ESM.[21] The presence of interfacial layer allowed a sustained release of antitumour drug for long term anticancer activity. The highly hydrophilic drugs show burst drug release. In order to improve the drug release of hydrophilic drugs, Oliveira *et al.* used a supramolecular assembly, in order to immobilize the drugs through host-guest interaction, and they fabricated ESM for drug delivery application.[22] Electrospun material with

[a] *Institut Européen des Membranes, UMR 5635 CNRS ENSCM Université Montpellier, Place Eugene Bataillon, F-34095 Montpellier cedex 5, France*
**sebastien.balme@umontpellier.fr*
[b] *Crystal Growth Centre, Anna University, Chennai, India, 600025.*
[c] *IRCM, Institut de Recherche en Cancérologie de Montpellier, INSERM U1194, Université Montpellier, Montpellier F-34298, France*

antiseptic properties exhibits also an important interest for implant and wound-dressing applications. These properties can be achieved by addition of silver nanoparticles [23] or antibacterial drugs [24]. Hence ESM are promising candidates to achieve tunable drug delivery for high therapeutic efficacy.

Stimuli responsive polymers are the typical class of materials encountered for drug delivery application. It is due to changes in conformation, phase or solubility by external stimuli such as pH, temperature, electric or magnetic fields. Designing pH sensitive drug carriers are more suitable to release the drugs: (i) along the gastrointestinal tract since the stomach is acid (pH=2) and the intestines is basic (pH=5-8),[25] (ii) in cancer cell since they display acidic extracellular pH[26] and variable pH in cellular compartments and (iii) in chronic skin, which wounds have pH values between 5.4 and 7.4.[27] Polymers which possess weak acids and bases such as carboxylic acid, amines, and phosphoric acid are ionizing at various pH environments which leads to conformation changes. Such a property is used for designing pH sensitive drug delivery carriers. Poly (amidoamine)/doxorubicin loaded polymer has been reported as a pH sensitive drug carrier for anticancer drug delivery applications.[28] Hence designing ESM using pH sensitive, biodegradable and nontoxic biopolymers for drug delivery can achieve high therapeutic effect.

This work aims at designing of ESM for antibacterial drug delivery applications. Our motivation was proposing a system only based on biological polymer to ensure a perfect biocompatilility. To make this, gelatin ESM was elaborated in order to understand the mechanism of drug release and the effect of pH and gelatin cross-linking upon drug release. Based on the results obtained from the model drug release profile, antibiotic loaded ESM were synthesized and tested against both Gram-negative and Gram-positive bacteria to assess the bactericidal behavior of this drug loaded ESM. The kinetics of bactericidal action is reported.

Experimental

Materials

Gelatin type A (48722-500G-F) from porcine skin (gel strength170-195 g Bloom), glacial acetic acid (320099), ethanol, 25% glutaraldehyde (GTA) (G6257), the buffers N-cyclohexyl-3-aminopropanesulfonic acid (Caps) (C2632), 2-(*N*-morpholino) ethanesulfonic acid (MES) (M8250), phosphate buffered saline (PBS) (P44717) tablet, and Agar (A1296) were purchased from Sigma-Aldrich. Rhodamine 640 (06400) was purchased from Exciton. Chlorhexidine (PHR1222) acetate was obtained from Fluka Chemicals. Lysogeny broth (LB) Miller culture medium (1214662) was purchased from Fischer Scientific. The chemicals were used without further purification. Water at 18 MΩ was produced by MilliQ (Millipore).

Preparation of spinning solution and electrospinning of gelatin/rhodamine and gelatin/drugs nanofibers

20% gelatin solution was prepared by dissolving gelatin in glacial acetic acid. The 0.1% rhodamine solution was prepared using 20% gelatin solution. The mixture was allowed to stir until rhodamine crystals were completely soluble. The obtained uniform solution of rhodamine/gelatin was used for electrospinning using a lab-made system.[29, 30] The gelatin/rhodamine solution was loaded in a 10 mL syringe. A syringe pump (KDS 100) was used to feed the solution through the needle (0.7 mm in diameter). The flow rate of the solution was fixed to 0.5 mL h^{-1} and the 25 kV power supplied using HPx 600 605 generator (Physical Instruments).[29] A piece of aluminum foil wrapped around the rotating machine (400 rpm) was used to collect the fibers. The electrospinning was carried out at 35°C (see supporting information SI1) under atmospheric air and the fibers were collected for 4 hours. The fibers prepared using 20% gelatin were denoted as G and the nanofibers prepared using gelatin/rhodamine were denoted as GR. The gelatin fibers loaded with drugs was synthesized using chlorhexidine acetate (1mg mL^{-1}) solution, which is prepared using 20% gelatin solution. The gelatin fibers prepared with chlorhexidine acetate were denoted as GD.

Cross-linking of the fibers

The obtained GR fibers were cross-linked using the vapor phase cross-linking method reported by Smith *et al.*.[31] The GTA solution of various concentrations 0.5%, 5% or 25% was prepared from 25 % stock solution, using 96 % ethanol as a solvent. The glutaraldehyde solution (20 mL) was added in a tightly closed container and 5cm x 5cm GR mats were allowed to equilibrate in glutaraldehyde vapors for cross-linking using different concentrations of 0.5%, 5% or 25%; these cross-linked fibers are denoted by 0.5GR, 5GR and 25GR respectively. The chlorhexidine loaded gelatin fibers were cross-linked with 5% glutaraldehyde and thereafter denoted as 5GD.

In vitro release of model drug molecule (rhodamine)

The release kinetics of rhodamine from 0.5GR, 5GR, and 25GR were analyzed. The kinetic of rhodamine release at buffer of various pHs (2, 5, 7 and 10) were carried out using 0.1 M of phosphate, MES, phosphate buffered saline and CAPS respectively. 10 mg of 0.5GR, 5GR and 25GR samples were suspended separately in 3 mL of each buffer. The rhodamine released from the ESM was quantified by absorbance measurements at 580 nm using UV-Visible spectrophotometer JASCO. The concentration of released rhodamine was recorded every 10 minutes, average results were reported for 3 different experiments (n=3). The 0.5GR suspended in various pHs (2, 5, 7 and 10) were denoted as 0.5GR pH2, 0.5GR pH5, 0.5GR pH7 and 0.5GR pH10 respectively. The experiment carried out using 5GR at different buffer pHs (2, 5, 7 and 10) were named 5GR pH2, 5GR pH5, 5GR pH7 and 5GR pH10 respectively. The analysis using 25GR ESM at various pHs (2, 5, 7 and 10) were referred as 25GR pH2, 25GR pH5, 25GR pH7 and 25GR pH10 respectively.

Characterization of the cross-linked gelatin ESM loaded with rhodamine or chlorhexidine

The FTIR spectra of cross-linked gelatin ESM loaded with rhodamine or chlorhexidine were recorded by the NEXUS instrument, equipped with an attenuated total reflection (ATR) accessory in the frequency range of 600-4000 cm^{-1}. The FTIR spectra were scanned at 2 cm^{-1} resolution and the signals were averaged.

The morphology of the as synthesized, cross-linked gelatin ESM loaded with chlorhexidine and model drug rhodamine as well as the cross-linked ESM after rhodamine release at various pHs was observed using HITACHI S4800 scanning electron microscopy system.

Bactericidal activity of 5GD ESM loaded with chlorhexidine drug

The antibacterial activity of the 5GD ESM loaded with chlorhexidine was assessed by agar diffusion methods.

Bacterial strains and culture media. Non-pathogenic Gram-negative *Escherichia coli* (K12 DSM 423, from DSMZ, Germany) and Gram-positive *Staphylococcus epidermidis* (CIP53.124, from Pasteur Institute Laboratory, Lyon, France) were chosen as surrogate microorganisms for bacterial contamination because of their difference in parietal composition linked to their Gram difference. Lysogeny broth (LB) Miller culture medium was used for cultivation, counting and agar diffusion tests. Agar was added to LB liquid medium (at a final concentration of 15.0 g L^{-1}) for the preparation of nutrient LB plates.

***Bacteria cultivation and plate preparation for agar diffusion tests*.** For each experiment, new bacterial cultures were prepared from frozen aliquots of *E. coli* and *S. epidermidis* stored at -20°C. The aliquots were first rehydrated separately in LB medium for 3h at 37°C under constant stirring (110 rpm). Then, the rehydrated aliquots were inoculated individually into fresh LB medium (5% v/v) and incubated overnight at 37°C under constant stirring (110 rpm) until the bacteria reached the stationary growth phase. Nutrient LB agar plates (9 cm diameter filled with 20 ± 0.1 mL of LB agar) were then inoculated separately with 1 ml of the *E. coli* and *S. epidermidis* cultures whose absorbance at 600 nm was adjusted to 0.21 ± 0.01 by dilution in LB broth.

Agar diffusion tests. Two tests were carried out: (A) a direct biofilm contact test in order to assess the bacterial removal in the biofilms by the 5GD sample and (B) an inhibitory growth test in order to characterize the ability of the 5GD sample to prevent bacterial growth around the sample. For these tests, samples of loaded 5GD (10 mg) were employed.

In the case of test (A), the freshly inoculated plates (obtained as previously described) were incubated overnight at 37°C to allow the formation of uniform biofilms on the nutrient surfaces. A 5GD sample was deposited respectively in the center of each *E. coli* and *S. epidermidis* biofilm grown onto the nutrient LB plates and the plates were then incubated at 37°C.

In the case of test (B), a 5GD sample was deposited respectively in the center of each plate that has just been inoculated with *E. coli* and *S. epidermidis* (as previously described) and the plates (containing bacteria and 5GD) were then incubated at 37°C.

For both tests, the activity of the 5GD samples was correlated to the appearance over time of clear zones around the samples. Clear zones were defined as zones where agar was clearly visible by comparison to the formed biofilm that recovered the agar. The clear zones corresponded to zones where bacteria were killed in the case of test A (direct biofilm contact test), and to zones where bacterial growth was inhibited in the case of test B (inhibitory growth test).

Each test was reproduced at least three times independently. For each experiment, negative control plates were run in parallel: plates with bacteria but without material (to confirm the 5GD action) and plates without bacteria or material (to check any cross-contamination).

Bacteria quantity removed (test A) or prevented from growing (test B). The bacteria quantity *N* (CFU) that was killed (test A) or prevented from growing (tests B) after 24 h of 5GD treatment was determined for both bacteria. The bacteria quantity N_0 (CFU) contained in the whole uniform biofilms formed onto the plates without material after 24 h of incubation was first counted by a plaque assay method. This allowed to determine the quantity of bacteria per surface unit $N_{0,surf}$ (CFU.cm^{-2}), by dividing the N_0 quantity by the total agar plate area (6.36 10^{-3} m^{-2}). Finally, knowing the clear zone area S (cm^2) measured at 24 h, the bacteria quantity *N* (CFU) was given by equation (1):

$$N = N_{0,surf}.S \qquad \text{(Equation 1)}$$

In order to determine N_0, nutrient LB agar plates were inoculated separately with *E. coli* and *S. epidermidis* cultures as for agar diffusion tests. Plates were then incubated 24 h at 37°C to form biofilms onto the surface. The biofilm overlayers containing the bacteria cells were individually scraped with an inoculation loop and collected into centrifuge tubes with 10 mL of PBS phosphate buffer (13 mM, pH = 7.0 ± 0.1). The collected bacteria were mixed with PBS and the obtained bacterial suspensions were washed by centrifugation (10 minutes at 12°C and 4300 rpm) to remove nutrients from the LB medium and thus to avoid further bacterial growth. After centrifugation, the bacterial pellets recovered were once again suspended separately in 10 mL of PBS. Each suspension was thereafter diluted by decades in PBS. Each dilution (1 mL) was spread on LB agar plates to allow the bacterial colonies to be counted. Negative controls (without bacteria) were performed in parallel for each counting. All plates were incubated at 37°C overnight and the colonies were counted. All experiments were performed three times and the whole bacteria quantity N_0 in the suspensions (thus in the biofilms) was calculated as the average of the colonies number divided by the 1 mL-spotted on the plates and multiplied by the total suspension

volume (10 mL), with the corresponding dilution factor taken into account.

pH of the bacterial cultures: evolution over time. In order to approach the pH range encountered in the bacterial biofilms formed onto LB plates, liquid cultures were prepared by individually inoculating 20 mL of liquid LB broth (initial pH = 7.0 ± 0.1) with 1 mL of *E. coli* and *S. epidermidis* cultures whose absorbance at 600 nm was adjusted to 0.21 ± 0.01. pH was then recorded in these liquid cultures (that were not agitated) over the maximal period of the experiments (72 h).

Cell culture

Human keratinocytes (HaCat) and NIH3T3 mouse fibroblasts were cultured using DMEM (Dulbecco's modified eagle medium) (Gibco 31331-028) medium with 10 % (v/v) fetal bovine serum (FBS)(Eurobio CVFSVF00-01) and 1% (v/v) penicillin/streptomycin (Gibco 15140-122) at 37°C in 5% CO_2. The cells were maintained in 10 cm diameter petri dishes and passaged using 0.05% Trypsin-EDTA (Gibco 25300-054).

Cell viability assay

The 5GD samples were cut into 0.6 mm diameter circles using the cork puncher and sterilized under UV light for 20 minutes. HaCat NIH3T3 cells ($1x10^3$ cells/well) were seeded in 96 well plates and allowed to attach for 24 hours. The sterilized samples were added in the wells and incubated for 1 and 8 days. Cell viability was analyzed using the MTT ((3-(4,5-Dimethylthiazol-2-yl)-2,5-diphenyl tetrazolium bromide) assay. Briefly the MTT reagent (0.5 mg/mL, 100 µL/well) was added onto the cells and incubated for 4h. The purple colored formazan crystals obtained after MTT reduction by living cells were solubilized using 100µL of DMSO (BDH prolab 23486.297) and the absorbance of the solution recorded at 560 nm using a Multiskan plate reader (Thermos, USA).

Results and Discussion

The electrospun fibers with rhodamine were characterized by SEM and FTIR before the kinetic studies of release. The rhodamine dye was chosen as model due to its strong absorbance in visible (580 nm) which is not in the range of tryptophan containing in gelatin. The SEM images of the uncross-linked (*i.e.* as synthesized) and cross-linked gelatin/rhodamine ESM are shown in Figure 1. The GR ESM as-synthesized were of 1.9 µm diameter. The diameter of the cross-linked ESM was increased up to 4.7 µm with the concentration of GTA cross-linker (Table 1) and decreased for 0.5GR ESM, due to the dehydration of gelatin fibers at high alcohol vapour concentration. The long time exposure with a high concentration of GTA vapours fused the neigbouring fibers and increased the diameter (Figure 1).

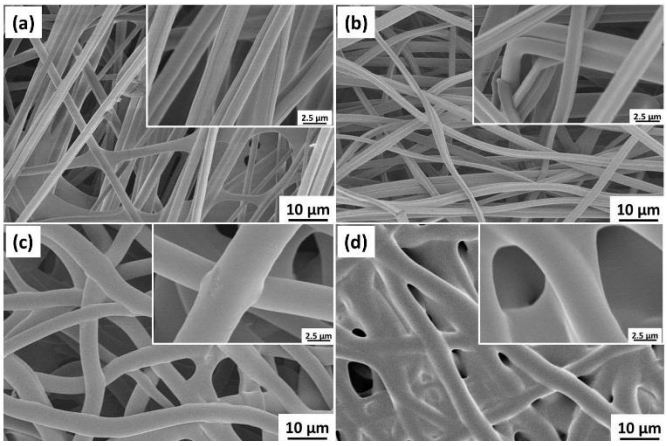

Figure 1: The scanning electron micrograph of (a) GR, (b) 0.5GR, (c) 5GR and (d) 25GR

Table 1. The size of as-synthesized and cross-linked rhodamine loaded ESM

Sample	Size (µm)
GR	1.9 ±0.4
0.5GR	1.4 ±0.2
5GR	4.5 ±0.9
25GR	4.7 ±0.7

The FTIR spectra of as-synthesized and cross-linked electro spun fibers are depicted in Figure 2. The characteristic peaks of amide I and II for gelatin are observed at 1635 cm^{-1} and 1523 cm^{-1} respectively. The shift of the amide II peak from 1523 cm^{-1} to 1532 cm^{-1} or 1528 cm^{-1} for GR samples can be assigned to amide groups induced by cross-linking of the gelatin molecules.

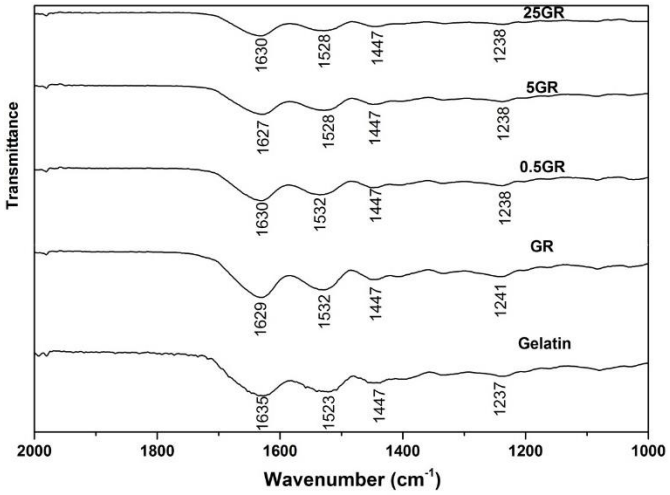

Figure 2. FTIR spectrum of as-synthesized and cross-linked Gelatin/Rhodamine ESM.

Effect of pH and cross-linking in rhodamine release from ESM

Gelatin is highly soluble in water, and, thus the stability of the ESM is improved by cross-linking with GTA. The vapour phase

crosslinking method was selected to avoid the loss of rhodamine. The effect of cross-linking of ESM on the release of rhodamine as well as fiber stability was investigated for different pHs from 2 to 10. The release kinetic is reported on Figure 3.

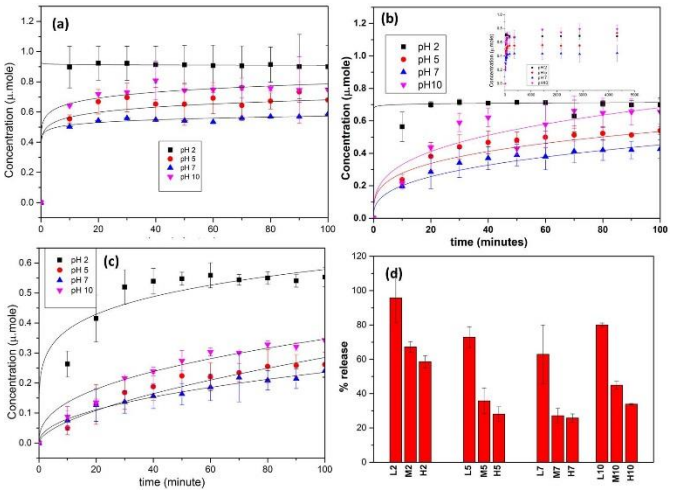

Figure 3: The rhodamine release profiles for cross-linked ESM at various pHs (a) 0.5GR, (b) 5GR, (c) 25GR and (d) Release percentage of rhodamine over 100 min.

Irrespective of the pH, the cross-linked ESM 0.5GR are highly soluble due to the poor cross-linking. It is related to the burst release of rhodamine. The loaded rhodamine concentration in the fibers was quantified by digesting the sample with HCl and used for calculating the percentage of release. At pH 2, the rhodamine release was maximum with 96% of release, which is higher than the release observed at pH 5 (73%), pH 7 (63%) and pH 10 (80%) ($p<0.05$) (Figure 3d). This evidenced that acidic pH enhances the solubility of gelatin, likely due to the hydrolysis of the cross-link function.[32, 33]

Contrary to 0.5GR mats, the 5GR and 25GR ESM are not completely soluble in buffer solution, since they were stabilized by cross-linking (Figure 3 (c,d)). At pH 2, the 5GR and 25GR released 67% and 58% of rhodamine respectively after 100 minutes (Figure 3d). These values were significantly lower than for 0.5GR. This evidenced that the cross-linking is an important parameter to tune the drug release. Indeed under 5% and 25% GTA vapors, a strong polymeric network is formed due to intercross-linking of gelatin molecules. This hinders the swelling of gelatin molecules and leads to decrease the release of rhodamine.

At pH 10, 5GR and 25GR released 45% and 34% of rhodamine respectively. The effect of cross-linking was enhanced at pH 5 and pH 7. Indeed, at pH 5, the 5GR showed 35% release whereas 25GR released 28%. At pH 7, 5GR and 25GR release 27% and 25% of rhodamine respectively. The rhodamine release thus increases for ESM treated at pH 2, pH 5 and pH 10 compared to pH 7. These results depict that at pH 7, the ESM are stable to the buffer and leads to a sustainable release of rhodamine through diffusion.

In order to describe the kinetics of rhodamine release from the gelatin ESM (Figure 3a to 3c), the experimental data obtained were fitted at equilibrium release using a model of power law (equation 2):

$$\frac{Mt}{M\infty} = Kt^n \qquad \text{(Equation 2)}$$

where t is the time, Mt and M_∞ are cumulative amount of drug released at time t and infinite time respectively, n is the exponent parameter, and K is a constant related to geometric characteristics. The M_∞ is calculated at equilibrium release. The value of parameter n is linked to the release process. Typically, if n=1, equation (2) follows zero order kinetics and drug release rate is independent of time. If n=0.5, the release is governed by the Fickian diffusion of the molecules inside the fiber. If n>0.5 leads to the non Fickian diffusion and the release under the study is governed by Fickian diffusion and also other processes such as corrosion or material degradation.[34-36] The parameters n and K resulting from the fitting of the model curves with the experimental curves are reported on Table 2.

Table 2. The fitting parameters n and K for rhodamine release from cross-linked ESM.

	0.5GR		**5GR**		**25GR**	
	n	**k**	**n**	**k**	**n**	**k**
pH 2	0.002 ±0.001	1	0.09 ±0.02	0.67	0.22 ±0.05	0.39
pH 5	0.07 ±0.03	0.76	0.42 ±0.02	0.15	0.49 ±0.06	0.11
pH 7	0.05 ±0.01	0.78	0.48 ±0.02	0.11	0.48 ±0.03	0.12
pH 10	0.05 ±0.02	0.80	0.48 ±0.03	0.18	0.49 ±0.05	0.10

For the 0.5GR gelatin/rhodamine ESM, the parameter n is lower than 0.1, irrespective of the pH. Thus the fickian model is not suitable for this ESM that undergoes complete dissolution in a short time.

Materials cross-linked with 5% and 25 % of glutaraldehyde (5GR and 25GR) exhibited n values close to 0.5 for pH 5, 7 and 10. It proves that rhodamine is released from these ESM according to the fickian diffusion. In addition, the values of constant related to geometric characteristics K are similar. This corroborates the close structure of fibers observed in SEM. At pH 2, the n value ranges from 0.09 (for 5GR) to 0.22 (for 25GR) depicts that rhodamine diffusion is not fickian. The high values of K and the discrepancy between the fitting with the model and the experimental data (figure 3) suggest a modification of fiber geometry and a degradation, and leading thus to an erosion of ESM are eroded at pH 2.

In order to confirm this assumption, the morphology of the fibers after release experiments was characterized by SEM (Figure 4 and 5). At pH 5, 7 and 10, both 5GR and 25GR ESM exhibited smooth fibers, evidencing that the pH has no influence on the fibers morphology. On the contrary, at pH 2, the SEM micrographs clearly showed (circled around the degraded fibers) that both 5GR (Figure 4a) and 25GR (Figure 5a) exhibited an eroded morphology. This can be assigned to the degradation of gelatin through hydrolysis at acidic pH.[32, 33] The fiber degradation also explains that rhodamine release is higher at pH 2 than at other pHs (Figure 2).

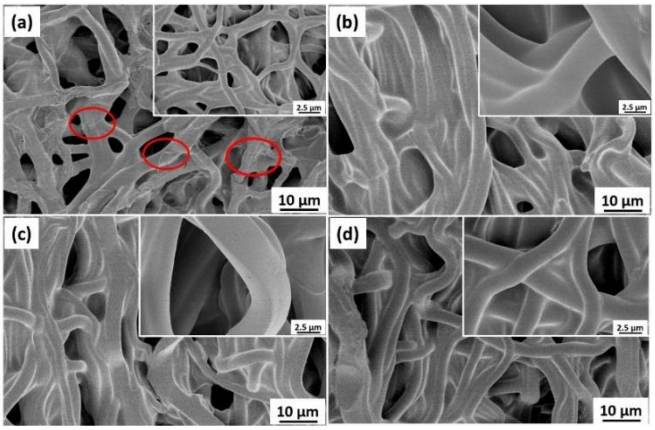

Figure 4: The scanning electron micrographs of ESM recovered after rhodamine release (a) 5GR pH 2, (b) 5GR pH 5, (c) 5GR pH 7 and (d) 5GR pH 10. The red circle indicates the erosion of fibers.

Chlorhexidine loaded into ESM

The gelatin ESM loaded with the antibiotic drug chlorhexidine were synthesized to analyse their antibacterial activity. From previous experiments, 5% GTA cross-linked ESM were chosen since the fiber are (i) stable at physiological pH and (ii) suited for a sustained drug release. The 5GD drug loaded ESM before cross-linking (*i.e.*, as-synthesized) (Figure 6a) and after cross-linking (Figure 6b) exhibited mean diameters of 3 ± 0.2 µm and 5.5 ± 0.5 µm respectively. The increase in the fiber size after cross-linking evidenced the cross-linking with neighboring fibers. The stability of the crosslinked fibers were highly influenced by pH. The 5 GD, 5 GR ESM at pH 5, 7, and 10 were stable for 7 days and the ESM equilibrated at pH 2 was completely separated into tiny fragments in 5 days and dissolved in 7 days. In addition, the fibrous morphology evidenced that the cross-linker concentration used was also suitable to preserve the morphology of the fibers.

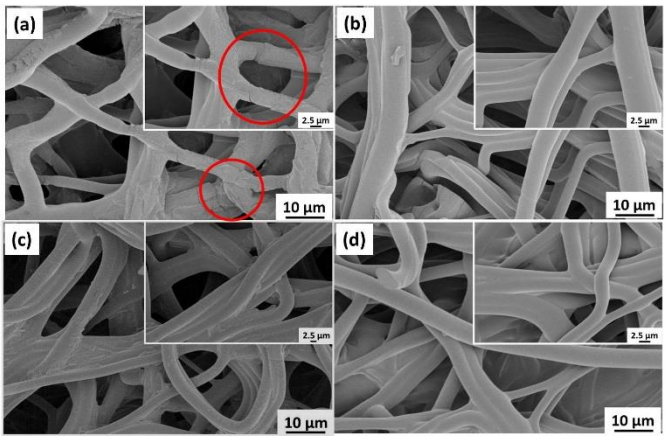

Figure 5: The scanning electron micrographs of ESM recovered after rhodamine release a) 25GR pH 2, (b) 25GR pH 5, (c) 25GR pH 7 and (d) 25GR pH 10. The red circle indicates the erosion of fibers.

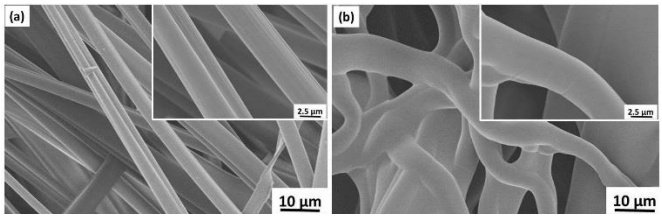

Figure 6: SEM micrographs of drug loaded ESM (a) as-synthesized, (b) cross-linked.

Bactericidal activity of 5GD electro spun mats loaded with chlorhexidine drug

Designing ESM with both biocompatible and antibiotic activity could be interesting for plaster application. In that frame, the antimicrobial activity of 5GD ESM loaded with chlorhexidine was characterized by two agar diffusion tests: (A) a direct biofilm contact test aiming to assess the material efficiency to remove bacteria on infected sites and (B) an inhibitory growth test whose objective was to assess the ability of the material to prevent treated areas from infection (*i.e.* bacterial contamination). For both tests, clear zones appeared around the 5GD material and their mean areas were recorded over time. An illustration of these clear zones is given in Figure 7.

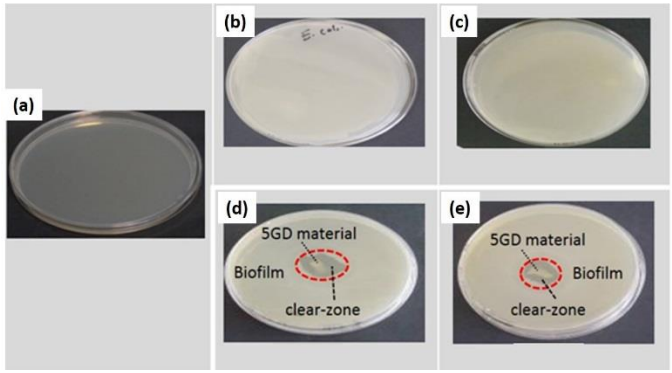

Figure 7: Illustrations of (a) nutrient agar plates without bacteria and without material, nutrient agar plates where uniform bacterial biofilms were formed without material: (b) for *E. coli* and (c) for *S. epidermidis*, and nutrient agar plates with clear zones appearing around the 5GD material and on the bacterial lawn (case of test B after 24 h of material treatment): (d) for *E. coli* and (e) for *S. epidermidis*.

Nutrient agar plates that were not inoculated (Figure7 (a)) showed a clear agar. On the contrary, nutrient agar plates that were seeded with bacteria exhibited uniform biofilms on their surfaces (Figure 7 (b,c)) giving a uniform turbidity to the plates. In presence of material (Figure 7(d,e)), clear zones were visible around the material that was deposited in the plate centers, for both tests (A and B) and both bacteria (*E. coli* and *S. epidermidis*). All of these zones globally showed a disk-shaped and the measurement over time of the mean diameter of these clear zones (averaged on three independent experiments) allowed determining their mean areas *S* over time (Figure 8).

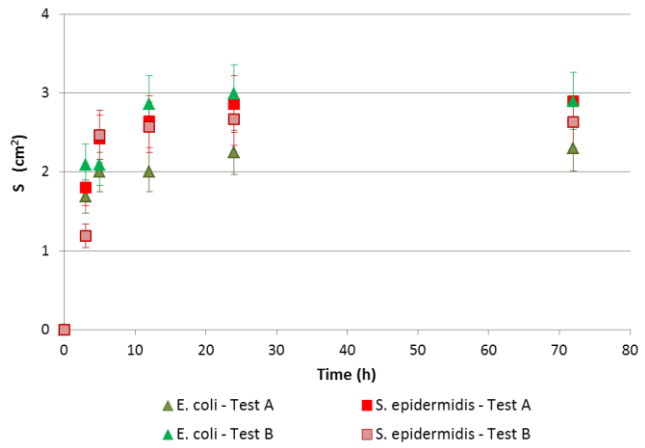

Figure 8: Evolution kinetics of the mean areas *S* (cm^2) of the clear zones formed around the 5GD material, for both tests (A and B) and for both bacteria (*E. coli* and *S. epidermidis*) (n = 3).

Irrespective of the test or the bacteria, all kinetics exhibited two phases (Figure 8): one phase for which the mean surfaces S increased (up to 5 or 12 h) followed by a leveling off of these areas (up to 72 h). In all cases, the clear zones reached stationary phase which depicts that no bacterial re-growth (for test A) or growth (for test B) occurred for at least 60 h (from 12 h to 72 h). These results put in evidence a sustainable release of the chlorhexidine drug from the 5GD material that achieved equilibrium from 12 h. These observations are consistent with the pH effect on the model drug release that was previously demonstrated (Figure 3b) as the pH of both bacterial cultures raises from 7.0 ± 0.1 (initially) to a constant value of 8.3 ± 0.2 (reached from 12 h and maintained up to 72 h).

Regarding *E. coli*, clear zones were larger for test B than for test A (Figure 8), that suggests that *E. coli* bacteria are more resistant during their stationary culture phase (test A) than during their growth phase (test B). On the contrary, no difference between results of tests A and B ($p>0.05$) was observed for *S. epidermidis*, which might be explained by a higher resistance of *S. epidermidis* bacteria during their growth phase due to its Gram-positive parietal structure.

Table 3: Bacteria quantity *N* (CFU) that was killed (test A) or prevented from growing (test B) after 24 h of 5GR treatment and bactericidal efficiency N/N_0 (%), where N_0 (CFU) is the whole bacteria quantity contained in the bacterial biofilms formed without material after 24 h of incubation (n = 3).

Test		*E. coli*	*S epidermidis*
	N_0 (CFU)	$2.4 \pm 0.2\ 10^{10}$	$4.2 \pm 0.1\ 10^{10}$
A	*S* (cm^2)	2.3 ± 0.3	2.9 ± 0.3
	N (CFU)	$8.6 \pm 0.2\ 10^{8}$	$1.1 \pm 0.1\ 10^{9}$
	N/N_0 (%)	4 ± 1	3 ± 1
B	*S* (cm^2)	3.0 ± 0.4	2.7 ± 0.3
	N (CFU)	$2.0 \pm 0.4\ 10^{9}$	$1.8 \pm 0.2\ 10^{9}$
	N/N_0 (%)	8 ± 2	4 ± 1

The bacteria quantity *N* (CFU) that was killed (test A) or prevented from growing (test B) on the inoculated plates after 24 h of 5GD treatment was determined for both bacteria (Table 3). The bacteria quantity N_0 (CFU) contained in the whole uniform biofilms formed onto the plates without material (Figure 7 (b,c)) after 24 h of incubation is also given in Table 3. In this study, the ratio N/N_0 (%) was defined as the bactericidal efficiency of the 5GD material.

The bacteria quantities N_0 in the biofilms formed on plates without materials were of the same order of magnitude for both bacteria (Table 3), which allowed a comparison between the 5GD bactericidal efficiencies for the two bacteria tested. Regarding test A, the bactericidal efficiency obtained toward *E. coli* and *S. epidermidis* were similar meaning that the 5GD material is able to remove as much as Gram-negative *E. coli* than Gram-positive *S. epidermidis* over 24 h of treatment. In the case of test B, the antibacterial efficiency was significantly higher (two folds more) against *E. coli* than against *S. epidermidis* (Table 3). This result might be attributed to a higher resistance of the Gram-positive bacteria during their growth phase, which is in accordance with the fact that there was no significant difference between the bactericidal efficiency against *S. epidermidis* either for test A (stationary phase) or B (growth phase).

The 5GD (10 mg) material loaded with chlorhexidine allowed thus the removal or the growth prevention of about 10^9 CFU on a mean area of 2.7 ± 0.3 cm^2 (Table 3), for two bacteria with two different Grams. The bactericidal activity of this loaded ESM appears to be very interesting as standardized contact tests were reported to assess the removal of 10^7 CFU on an area of 0.5 cm^2 (corresponding to a disc of 8 mm diameter).[37] Moreover, the antibacterial action of the 5GD material loaded with chlorhexidine is rapid (with a significant effect visible from 3 h of treatment) and persistent over at least 72 h (Figure 8). The antibacterial activity of the ESM against the gram positive and gram negative bacteria clearly evidences that the integrity of the drug is not significantly affected by the high voltage during the electrospinning. Hence these type of ESMs are suitable material for plaster application so that to treat infected sites or to prevent infection.

Cell viability of drug loaded ESM.

Keratinocytes play vital role in wound healing by differentiating into neoepidermis and covering the wound surface. Fibroblasts improve wound healing by forming the collagen and extra cellular matrix. Hence understanding the biocompatibility of the ESM with these two types of cells was essential. The biocompatibility of the scaffolds was analyzed after 1 and 7 days of culture using Hacat human keratinocytes and NIH3T3 mouse fibroblasts. As shown in Figure 9, no significant difference in cell viability was observed at 1 day for both cell types. In the presence of ESM, the cell viability decreased by 25 to 30% after 7 days of culture as compared to control cells. However, for both cell types, a significant increase in proliferation was observed between 1 and 7 days even in the presence of the ESM demonstrating their biocompatibility.

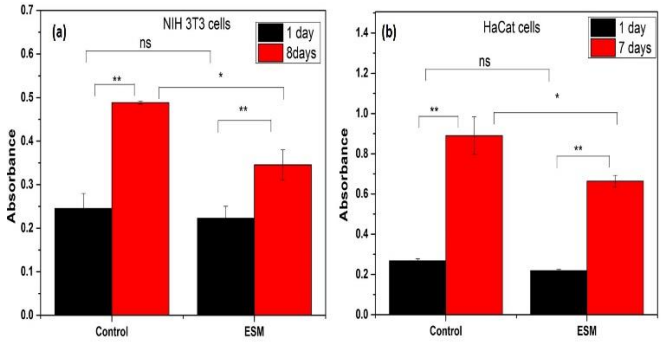

Figure 9: Cell viability of chlorhexidine loaded ESM. ns- no significant change, * P<0.05, ** p<0.005

Conclusions

Gelatin ESM for drug delivery applications were synthesized and tested for chlorhexidine release against bacteria. The mechanism of drug release from the ESM and the stability of fibers were first studied using a rhodamine dye. This study clearly shows that the drug release from the ESM is tuned by varying the cross-linking degree of the ESM. The synthesized ESM showed also interesting pH effect on drug release, which can be useful for drug delivery application. In particular, the ESM allows burst drug release at acidic pH 2 and sustained drug release at pH 7, which shows that the ESM are promising candidate for burst as well as sustained drug release, depending on environment. The 0.5% GTA cross-linked samples are poorly stable which leads to maximum release. On the contrary, 5% and 25% GTA cross-link samples follows fickian diffusion at pH 5, 7 and 10 whereas at pH 2 the drug release is controlled by erosion. By determining the suitable cross-linker concentration for sustained drug release (5% GTA), ESM loaded with chlorhexidine antibiotic were synthesized. It was proved that these synthesized ESM are highly active against *E. coli* and *S. epidermidis* at pH 7-8, either to remove bacteria or to prevent their growth. Finally, the biocompatibility of drug loaded ESM was analysed using keratinocytes and fibroblasts and data indicated that the ESM were highly biocompatible. Drug loaded Gelatin ESM are promising material for wound-dressing with antibiotic properties.

Acknowledgements

S. N. benefits of Svagaata Fellowship (Erasmus Mundus Program, European Union), Authors thank Gael H. Nguyen (IEM, Montpellier) for English proof-reading. This work was partially supported by the European Institute of Membrane by health project (PS1-2015).

References

1. T. Yu, X. Liu, A.-L. Bolcato-Bellemin, Y. Wang, C. Liu, P. Erbacher, F. Qu, P. Rocchi, J.-P. Behr and L. Peng, *Angewandte Chemie International Edition*, 2012, **51**, 8478-8484.
2. W. Lin and D. Kim, *Langmuir*, 2011, **27**, 12090-12097.
3. S. Rana, A. Gallo, R. S. Srivastava and R. D. K. Misra, *Acta Biomaterialia*, 2007, **3**, 233-242.
4. S. Lv, M. Li, Z. Tang, W. Song, H. Sun, H. Liu and X. Chen, *Acta Biomaterialia*, 2013, **9**, 9330-9342.
5. X. Ma, K. T. Nguyen, P. Borah, C. Y. Ang and Y. Zhao, *Advanced Healthcare Materials*, 2012, **1**, 689-689.
6. W. Friess, *European Journal of Pharmaceutics and Biopharmaceutics*, 1998, **45**, 113-136.
7. Y. Marois, N. Chakfé, X. Deng, M. Marois, T. How, M. W. King and R. Guidoin, *Biomaterials*, 1995, **16**, 1131-1139.
8. K. R. Stevens, N. J. Einerson, J. A. Burmania and W. J. Kao, *Journal of Biomaterials Science, Polymer Edition*, 2002, **13**, 1353-1366.
9. W. Meng, Z.-C. Xing, K.-H. Jung, S.-Y. Kim, J. Yuan, I.-K. Kang, S. Yoon and H. Shin, *J Mater Sci: Mater Med*, 2008, **19**, 2799-2807.
10. A. K. Bajpai and J. Choubey, *J Mater Sci: Mater Med*, 2006, **17**, 345-358.
11. S. K. Jain, Y. Gupta, A. Jain, A. R. Saxena, P. Khare and A. Jain, *Nanomedicine: Nanotechnology, Biology and Medicine*, 2008, **4**, 41-48.
12. E. Lee, S. Khan, J. Park and K.-H. Lim, *Bioprocess Biosyst Eng*, 2012, **35**, 297-307.
13. E. Leo, M. Angela Vandelli, R. Cameroni and F. Forni, *International Journal of Pharmaceutics*, 1997, **155**, 75-82.
14. M. Nahar, D. Mishra, V. Dubey and N. K. Jain, *Nanomedicine: Nanotechnology, Biology and Medicine*, 2008, **4**, 252-261.
15. T. Yeh, Z. Lu, M. G. Wientjes and J. S. Au, *Pharm Res*, 2005, **22**, 867-874.
16. H.-C. Liang, W.-H. Chang, K.-J. Lin and H.-W. Sung, *Journal of Biomedical Materials Research Part A*, 2003, **65A**, 271-282.
17. W. Liu, S. Thomopoulos and Y. Xia, *Advanced Healthcare Materials*, 2012, **1**, 2-2.
18. Z. X. Meng, X. X. Xu, W. Zheng, H. M. Zhou, L. Li, Y. F. Zheng and X. Lou, *Colloids and Surfaces B: Biointerfaces*, 2011, **84**, 97-102.
19. J. Wei, J. Hu, M. Li, Y. Chen and Y. Chen, *RSC Advances*, 2014, **4**, 28011-28019.
20. D.-G. Yu, X.-Y. Li, X. Wang, J.-H. Yang, S. W. A. Bligh and G. R. Williams, *ACS Applied Materials & Interfaces*, 2015, **7**, 18891-18897.
21. X. Zhao, J. Zhao, Z. Y. Lin, G. Pan, Y. Zhu, Y. Cheng and W. Cui, *Colloids and Surfaces B: Biointerfaces*, 2015, **130**, 1-9.
22. M. F. Oliveira, D. Suarez, J. C. B. Rocha, A. V. N. de Carvalho Teixeira, M. E. Cortés, F. B. De Sousa and R. D. Sinisterra, *Materials Science and Engineering: C*, 2015, **54**, 252-261.
23. A. M. Abdelgawad, S. M. Hudson and O. J. Rojas, *Carbohydrate Polymers*, 2014, **100**, 166-178.
24. A. R. Unnithan, N. A. M. Barakat, P. B. Tirupathi Pichiah, G. Gnanasekaran, R. Nirmala, Y.-S. Cha, C.-H. Jung, M. El-Newehy and H. Y. Kim, *Carbohydrate Polymers*, 2012, **90**, 1786-1793.
25. A. T. Florence and D. Attwood, *Physicochemical Principles of Pharmacy*, Pharmaceutical Press, 2006.

26. E. K. Rofstad, B. Mathiesen, K. Kindem and K. Galappathi, *Cancer Research*, 2006, **66**, 6699-6707.
27. J. Dissemond, M. Witthoff, T. C. Brauns, D. Haberer and M. Goos, *Hautarzt*, 2003, **54**, 959-965.
28. N. Lavignac, J. L. Nicholls, P. Ferruti and R. Duncan, *Macromolecular Bioscience*, 2009, **9**, 480-487.
29. A. A. Chaaya, M. Bechelany, S. Balme and P. Miele, *Journal of Materials Chemistry A*, 2014, **2**, 20650-20658.
30. M. Bechelany, M. Drobek, C. Vallicari, A. Abou Chaaya, A. Julbe and P. Miele, *Nanoscale*, 2015, **7**, 5794-5802.
31. Y. Z. Zhang, J. Venugopal, Z. M. Huang, C. T. Lim and S. Ramakrishna, *Polymer*, 2006, **47**, 2911-2917.
32. R. P. Gullapalli, *Journal of Pharmaceutical Sciences*, 2010, **99**, 4107-4148.
33. R. J. Croome, *Journal of Applied Chemistry*, 1953, **3**, 280-286.
34. P. I. Lee, *Journal of Controlled Release*, 1985, **2**, 277-288.
35. T. Higuchi, *Journal of Pharmaceutical Sciences*, 1963, **52**, 1145-1149.
36. P. L. Ritger and N. A. Peppas, *Journal of Controlled Release*, 1987, **5**, 23-36.
37. R. Glaser, J. Harder, H. Lange, J. Bartels, E. Christophers and J.-M. Schroder, *Nat Immunol*, 2005, **6**, 57-64.

Graphical Abstract